Technical Progress in HTS Magnetic Bulk Application Development

F. N. Werfel, U. Floegel-Delor, T. Riedel, R. Rothfeld, P. Schirrmeister, D. Wippich, R. Koenig

***Abstract*—Experimental studies and theoretical modeling of High Temperature Superconductor (HTS) magnetic bulk applications are conducted and reported. The magnetic force density as a function of the magnet superconductor separation in the mirror image FEM 2D picture shows a strong dependency on the distance and PM mass. The behavior contrasts all attempts of generating high magnetic levitation forces with a minimum of material effort. An optimum configuration PM HTS coupler has been designed and built for a 300 mm wafer spin test apparatus. With rotational speeds up to 1500 rpm a safe operation and handling the imbalance of the wafer spin clutch by passing the resonance speed at 370 rpm is investigated. The smart rotor rotation is studied to drive a half-wave plate of a polarization apparatus to detect cosmic microwave radiation safely through resonances and imbalance effects.**

***Index Terms* – HTS bulk magnet application, FEM, magnetic wafer spin clutch, coupling phenomena, resonance effects, CMB polarization, and soft rotation.**

I. Introduction

The basic parameters of magnetic levitation are well understand and are described in a number of excellent reviews and reports [1]-[4]. Technological skills as efficient cryogenics, minimal rotational loss or damping properties to utilize the stable levitation in high sensitive apparatus has hitherto been less carefully investigated. We investigate and report about the construction of HTS thrust bearings to support a 300 mm spin wafer magnetic clutch and rotate a half-wave plate of a polarimeter for measuring cosmic microwave background (CMB) radiation. A HTS magnetic clutch in semiconductor wafer processing is a new and unique technique. Equally effective is the soft continuous rotation of a half - wave plate at liquid Helium temperature for modulating the polarization of incident cosmic background radiation. In both cases a number of requirements and advantages favor the use of HTS bearing as low rotational friction, no wear and the absence of any motion control. In both applications reported here, the trapped magnetic flux capability in bulk HTS is basic for the function.

Very recently, an extremely high trapped magnetic field of 17.6 T between a stack of two GdBCO samples has been successfully demonstrated by the Cambridge group [5]. Following their conclusions, the limitations of maximum fields are not determined by electric parameters of the HTS samples it seems rather a question of the mechanical stability of the material.

Similar specific are the technical requirements of magnetic levitation to support and to spin a 12-inch silicon wafer in a hermetically closed semiconductor apparatus. The shaft-less rotor equipment is designed, built and tested to reduce particle generation during high – sensitive wet and dry wafer spin processes. As a key feature the rotational control of the spinning wafer in its rotor dynamics and high precision is analyzed. Loading and de-loading the wafer uses an external robot system. In a first step a bearing of comparable size was modified to a magnetic coupling or clutch system. As a great advantage the magnetic clutch is capable to support and spin the wafer simultaneously and allows an exact control of the motion in all operational phases (processing, cleaning, drying).

II. Materials

A Optimum magnetic biasing

From the viewpoint of force functionality a bulk superconductor basically acts as a passive element. An external magnetic field whether it is generated from permanent magnet (PM) or coil will interact with the HTS. Either the magnetic field is screened perfectly by surface currents (diamagnetic screening) or the magnetic flux is trapped by pinning forces within the bulk. Meissner effect is usually ignored by PM - HTS force consideration because of its weakness (a few tenths of a percent). Curiously, levitation experiments and pictures showing a “flying” PM above a cooled HTS block are still insistently described as Meissner effect. However, the Meissner part is very weak, it’s close to

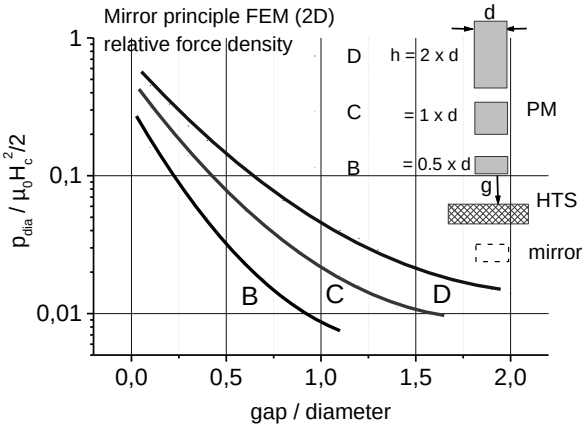

Fig. 1. Superconductor magnet interaction: 2D FEM mirror principle calculation for designing PM configuration

Manuscript received August 12, 2014

F. N. Werfel , U. Floegel - Delor, T. Riedel, R. Rothfeld, D. Wippich, P. Schirrmeister and R. Koenig are with the Adelwitz Technologiezentrum GmbH (ATZ), Adelwitz, Germany, Phone +49 34222 45200, e-mail: werfel@t-online.de;

one hundred percent pinning forces that levitates a PM several centimeter stably above a bulk HTS.

For efficient application the magnitude of magnetic forces determines the necessary amount of HTS material and design. Thereby magnetic circuits obey the basic laws of electricity and magnetism, in detail the rules for conservation of magneto-motoric force. The PM property depends on the energy product $(BH)_{max}$ with an operating point dependent on the application. In most levitation cases the magnetic flux density being about half of the remanence force $B_{PM} \sim B_r/2$ determines the performance. It follows the basic experience that higher magnetic forces require larger magnetic flux density excitations equivalent to a larger volume and mass input of magnet material.

To investigate this relation detailed either an analytical [6]-[7] or at least semi-quantitative picture is helpful. A first and useful step is the so –called mirror image concept in figure 1. In this picture one assumes an ideal diamagnetic superconductor response to an external magnetic excitation. The magnetic interaction is thereby considered as a one-to-one reaction. In this model both the field magnitude of the response excitation as well as the position of the diamagnetic image follow perfectly the origin. The horizontal stability shows some itinerancy due to edge effects of the superconductor dimension.

In figure 1 FEM calculations of permanent magnet interaction with a HTS in a principle 2D mirror image are shown. The gap distance is a simple ratio of the diameter of the PM giving three curve parameters for the obtained relative diamagnetic pressure. The resultant force density is referenced to the magnet performance/ filling factor by increasing the PM height as half, equal and double the gap. The calculated curves give a first approach of the expected levitation performance dependent on magnet size and distance of the magnet from the superconductor.

B Design of HTS bulk

The second part of the progress in HTS bearing and levitation is the superconductor. Figure 2 displays the concept and geometry of seeded REBCO melt textured growth. Typical bulk stator geometries displayed in the lower part of figure 2 represents a 300 mm YBCO ring (left) with orthogonal c axes and a 80 mm journal-type cylinder with radial c axes (right). Both components consist of assembled, glued and machined single grain bulks.

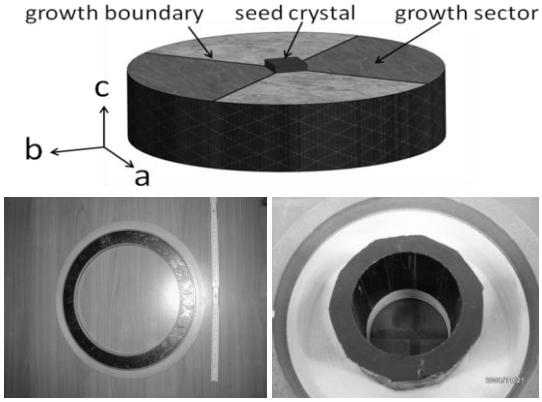

Fig. 2. HTS bulk melt texturing technique (top); well oriented thrust –type and journal- type YBCO stator components.

A geometrical condition for generating high currents and high trapped field values is an optimum geometry of the magnetic field component which should be orthogonal to the crystallographic a, b plane of YBCO single grain bulk. Figure 3 displays measurements of different YBCO cylinders with a c axis orientation parallel and perpendicular to the radial magnetic flux distribution. Surprisingly, the axial force seems to be less sensitive to the crystal orientation of the YBCO stator for displacement values up to 4 mm. The polycrystalline stator exhibits lower magnetic forces as expected.

While stable external levitation is a prominent performance of bulk superconductors the same forces act on the inner structure of the material too. Magnetic energy and pressure behave much like mechanical work. The force density exerted on a unit superconductor volume depend on the induced current density **j** and the 'magnetic induction' ***B*** or the field inside the superconductor,

$$\boldsymbol{j}\,\boldsymbol{x}\,\boldsymbol{B} = \frac{1}{\mu_0}(\nabla x\,\boldsymbol{B})x\,\boldsymbol{B} = grad\left(\frac{B^2}{2\mu_0}\right) + \boldsymbol{B}\,grad\left(\frac{B}{\mu_0}\right) \quad (1)$$

The first term is the magnetic pressure whereby the second term corresponds to a tension of B/μ_0 along the lines of force.

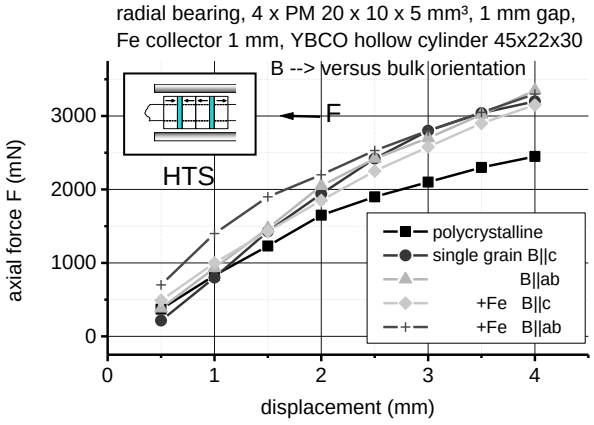

Fig. 3. Measurement of the YBCO orientation relative to magnetic flux direction together with polycrystalline YBCO stator

III. HTS MAGNETIC WAFER CLUTCH

A Design

Magnetic couplings and clutches are well known in modern machinery to transfer forces or momentum forces from one element to another one without mechanical connection. However, these types of coupling are unstable in at least one geometrical direction. Either the magnets attract each other or show repulsive forces. Therefore, magnetic bearings made of permanent magnets need an additional stabilization either in radial or in axial direction. In contrast, the interaction between a superconductor and magnet result in self-stabilization without additional effort. Based on the concept of trapped flux we designed and built a wafer clutch and used magnetic forces between permanent magnet and HTS bulk elements. Cooling of the HTS is performed using a developed rotatable vacuum cryostat with LN_2 cryogenics. To maintain a homogeneous

moment of inertia of the cryostat the dynamics of LN_2 liquid in the cryostat during the rotation has been studied. The uncontrolled LN_2 distribution and the resulting momentum forces during acceleration and slowing-down the cryostat were especially critical for a save wafer spin operation. With the results of experiments and calculations we solved the challenge robust cryogenics by utilizing principles of ship construction. The cryostat was subdivided into a shell and chamber structure.

The stator consists of a superconductor ring axially spaced to the rotor with a corresponding axial gap. Figure 4 shows the magnetic wafer clutch consisting of a PM rotor part and the ring-shaped YBCO in the rotatable cryostat. Both are operating magnetically through the bottom of a semiconductor processing chamber. The silicon wafer is fixed on a magnetic wafer carrier and spin without any mechanical contact in the sealed chamber. The processing chamber is fabricated in the shape of a Kloepper bottom to withstand vacuum or pressure forces at lowest wall thickness. The material of the chamber is high-grade non-magnetic CuAl - alloy known from submarine construction.

B Function

By consideration the force density dependence of Fig. 1 we use the mirror model PM configuration with height-to-lateral dimension of 1:1. The 12 cuboid-shape PM pairs share the outer magnetic clutch part that comprises of an YBCO annular ring. The ring is mounted of individual YBCO blocks machined to fit the ring shape. After field cooling (fc) the cryostat is driven by a motor on a shaft and the wafer turn table rotates together with the semiconductor wafer. With such a magnetic wafer spin apparatus it is possible to process a semiconductor at elevated temperatures up to 200°C, higher pressure and without possible induction of dangerous currents in electric circuits.

According to figure 1 the transferable torque force can be increased by larger size, smaller distance to the HTS bulk, and higher pole number of the designed magnet circuit. For smaller twist angles of 5° – 8° at fixed stator the rotor has a tendency to switch back into original position. This re-tractable force is the limit for the applicable guidance force to accelerate or break the rotor. Even, if the driven rotor is removed from the process chamber the pinning forces in the superconductor allow an exact re-positioning of the rotor with reference to the driving rotor position. The technical data are collected in Table I. A rotor exchange with similar magnet circuit can be performed and repeated as long as the superconductor is under cryogenic conditions.

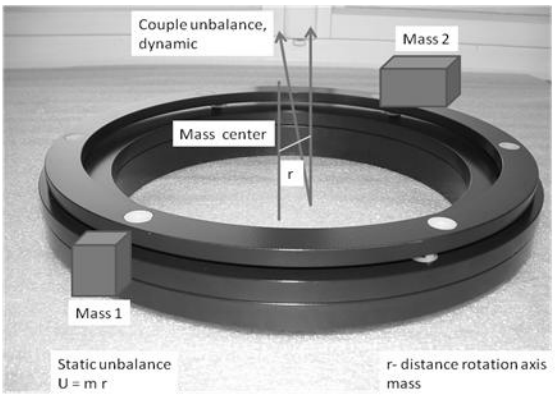

Fig. 4. 300 mm wafer spin rotor and unbalance effects

Table I Wafer carrier parameters

Excitation B		12 x PM
PM – HTS distance		12 mm
Axial stiffness	S_{ax}	16 N/mm
Radial stiffness	S_{rad}	7 N/mm
Rotational stiffness	(arc)	4 N/mm
Moment of inertia	Φ	0.0673 kgm²(carrier)
	Φ_t	0.42 kgm² (total)
Rotational moment		2.1 Nm (carrier)
Dynamic moment M		13.2 Nm
Spin-up 1500 rpm		time 5 s
Motor power ω x M		2 kW
Maximum speed		1500 rpm

C Wafer carrier in the critical rpm

The critical speed of the wafer carrier occurs at about 370 rpm. With this value the calculated radial stiffness is k_r = 6 N/mm. For a safe operation it is necessary to pass the critical rpm region in a short time to prevent large elongating amplitudes of the carrier. To obtain a first approximation how fast one should pass the critical rpm and to limit the magnitude of the amplitude we consider the rotor dynamic equation

$$\frac{d^2R}{dt^2} + \left(\frac{D}{m}\right)\frac{dR}{dt} + \omega R = \varepsilon\Omega^2 e^{i(\omega t+\beta)} \quad \omega = \left(\frac{S}{m}\right)^{1/2} \quad (2)$$

Solving this equation delivers a homogeneous and a particular solution for the imbalance excitation. According to the solutions the orbit radius R increases with the rotational speed ω, at the beginning rather fast followed by a gradual deceleration to the maximum value of the amplitude in the resonance. The orbital radius in the resonance is $R_{res} = \varepsilon / 2\ D$ with the eccentricity ε and the damping factor D.

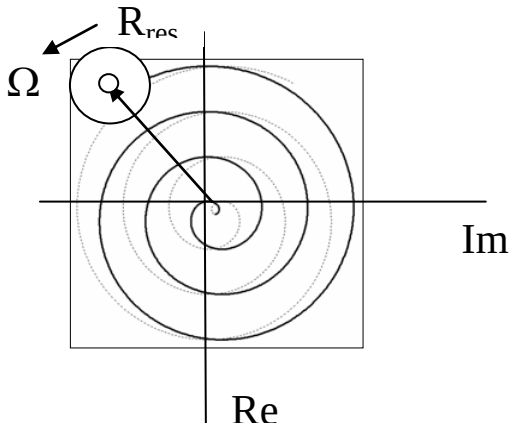

Fig. 5. Orbital radius vector under resonance imbalance excitation followed archimedic helix geometry

In the limit case of no damping (D = 0) the center of the wafer ring as virtual axis follows an archimedic helix. The (virtual) axis point moves at the resonance frequency on an

orbit of the shape of an Archimedean spiral. Geometrically the resultant curvature is described by a vector rotating with a constant angular velocity and a continuous increase of the vector value (length) as it is shown in figure 5. In the absence of any damping the magnitude of the orbital radius of the wafer carrier shown in figure 4 with an assumed eccentricity of 0.2 mm can be estimated within one second (1 s) to

$$|R_{res}| = ½\ 0.2\ \text{mm}\ 2\pi\ (370/60\text{s})\ 1\ \text{s} = 3.9\ \text{mm} \quad (3)$$

In this case the wafer ring would touch the chamber housing and needing a distinct damping behavior.

The quantity U = m·r is known as unbalance and the resulting centrifugal force is the product of unbalance and angular velocity squared. While unbalance forces ($F_{centrifugal}$) increase rapidly with speed, the unbalance quantity itself (m·r) does not change at all.

$$F_{centrifugal} = m \cdot r \cdot \omega^2 = U \cdot \omega^2 \quad (4)$$

In fast- rotating machines the unbalance is a combination of static and dynamic unbalance outlined in figure 4.

IV. POLARIZATION EXPERIMENT WITH HTS BEARING

Polarization experiments of the Cosmic Microwave Background (CMB) uses HTS bearings because of advantages over mechanical bearings having stick-slip friction effect that induce vibrations. The vibrations deposit mechanical energy in the detectors and cause wires to vibrate thereby inducing excess noise. The best technique currently available for modulating the polarization of the incident radiation is by

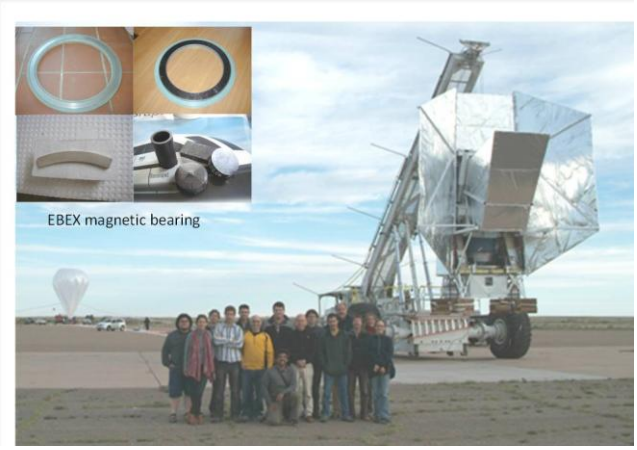

Fig. 6. Helium balloon borne EBEX polarization experiment for detection of cosmic microwave radiation (U. Minnesota).

rotation a half wave plate (HWP). The radiation field encodes new and valuable information about the earlier development phases of galaxies. When a HWP is placed in the path of the incident light and turned at a rotation frequency *f*, the polarization vector of the output radiation rotates at a frequency of 4*f*. The signal recorded by a Bolometer detector is modulated at a frequency of 4*f* and standard lock-in techniques to extract its magnitude.

We have developed thrust magnetic bearings for use with polarization experiments that is based on magnetic levitation HWP above HTS rings in sizes 200 – 400 mm. The HWP is mounted on corresponding assembled PM ring as rotor. The apparatus were designed to fit both in balloon borne bolometric experiments as well as stationary in European Southern Observatory ESO operating in the Atacama Desert region of Chile. The airborne experiment is displayed in figure 6 with the Minnesota group of S. Hanany [8]. The stator parts of the magnetic thrust bearings consist of single grain YBCO bulks fitted in ring shape and supported by annular holders of G-10 or brass. Both materials are nonmagnetic.

The magnetic stiffnesses of a 300 mm HTS thrust bearing operated at a height of 38 km in the airborne experiment of figure 6 were determined to 80 N/mm both in axial and radial direction at 4 mm gap distance. At a larger distance of 10 mm between stator and rotor we measured 43 N/mm axially but only 12 N/mm radially. Similarly to the wafer spin apparatus rotation specific parameters play a dominant role: solid state critical rpm, stiffness, damping and losses.

The rotational drag or friction depends on the magnetic distance and the homogeneity of the circular magnetization of the assembled PM ring with the HWP integrated. In figure 7 the recorded magnetic flux variation is measured above the rim center of the assembled PM ring. Direct on the surface the maximum deviation is about 6 mT over one rotation. At 2 mm distance the inhomogeneity is reduced to 4 mT which corresponds to about 1% of the total magnetic flux.

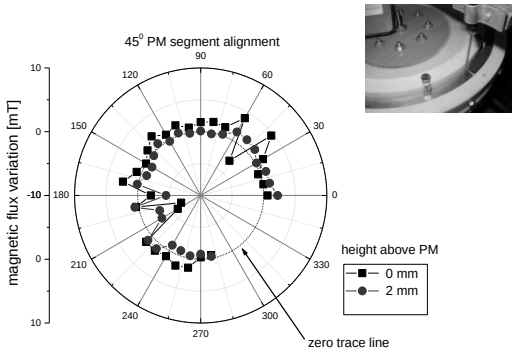

Fig. 7. Recorded inhomogeneity of the assembled magnet ring carrying a half- wave plate for cosmic microwave polarization; Hall probe measurement (insert).

V. CONCLUSIONS

Large-diameter HTS magnetic bearing and magnetic clutch configurations have been investigated for optimum magnet biasing and smart rotational behavior. 2D FEM calculations give a first approach for design and construction. The levitation experiments with a new HTS magnetic wafer spin clutch for semiconductor processing exhibit critical issues. The combination of unbalance and rotor dynamics requires damping and sufficient fast acceleration. Polarization experiments of cosmic microwave background radiation utilize the soft rotation performance of HTS bearing as low noise, low vibration and ultra-low friction.

REFERENCES

[1] E. H. Brandt, "Rigid levitation and suspension of high-temperature superconductors by magnets*", Am. J. Phys.* 58, 43- 49, 1990.

[2] F. C. Moon, "Superconducting levitation- Applications to Bearings and Magnetic Transportation" *J. Wiley and Sons*, New York, 1994

[3] J. R. Hull, "Superconducting bearings" *Supercond. Sci. Technol.* **13** R1 - R15, 2000.

[4] F. N. Werfel, U. Floegel – Delor, R. Rothfeld, T. Riedel, G. Goebel, D. Wippich, and P. Schirrmeister," Superconducting Bearings, Flywheels and Transportation" *Supercond. Sci. Technol.* 25, 014007, 2012.

[5] J. H. Durrell, A.R. Dennis, J. Jaroszynski, M. D. Ainslie, K.G.B. Palmer, Y.- H. Shi, A. M. Campbell, J. Hull, M. Strasik, E. E. Hellström and D. A. Cardwell, A trapped field of 17.6 T in melt – processed bulk Gd-Ba-Cu-O reinforced with shrink-fit steel, *Supercond. Sci.Technol. 27, 082001, 201.*

[6] C. Navau, N. De-Valle, A. Sanchez, Macroscopic Modeling of Magnetization and Levitation of Hard Type-II Superconductors: The Critical-State, Model, *IEEE Trans. Appl. Supercond. vol.32, no.1, 8201023, 2013.*

[7] G. T. Ma, Consideration on the Finite-Element Simulation of High – Temperature Superconductors for Magnetic Levitation Purpose, *IEEE Trans. Appl. Supercond. vol. 23 no 5, p. 3601609, 2013.*

[8] S. Hanany, T. Matsumura, B. Johnson, T. Jones, J.R. Hull, and K.B. Ma, "A cosmic microwave background polarimeter using superconducting bearings", *IEEE Trans. Appl. Supercond.*13,2128- 2133, 2003.